Forchheimer Flow to a Well Considering Time-Dependent Critical Radius

A revised Technical Note prepared for *Hydrology and Earth System Sciences*

Quanrong Wang[1], Hongbin Zhan[1,2*], and Zhonghua Tang[1]

[1]School of Environmental Studies, China University of Geosciences, Wuhan, Hubei, 430074, P. R. China, Email: wqr88@126.com (Quanrong Wang), zhhtang@cug.edu.cn (Zhonghua Tang)

[2]Department of Geology and Geophysics, Texas A& M University, College Station, TX 77843-3115, USA, Email: zhan@geos.tamu.edu

(*Corresponding author)

Abstract:

Previous studies on the non-Darcian flow into a pumping well assumed that critical radius (R_{CD}) was a constant or infinity, where R_{CD} represents the location of the interface between the non-Darcian flow region and Darcian flow region. In this study, a two-region model considering time-dependent R_{CD} was established, where the non-Darcian flow was described by the Forchheimer equation. A new iteration method was proposed to estimate R_{CD} based on the finite-difference method. The results showed that R_{CD} increased with time until reaching the quasi-steady state flow, and the asymptotic value of R_{CD} only depended on the critical specific discharge beyond which flow became non-Darcian. A larger inertial force would reduce the change rate of R_{CD} with time, and resulted in a smaller R_{CD} at a specific time during the transient flow. The difference between the new solution and previous solutions were obvious in the early pumping stage. The new solution agreed very well with the solution of previous two-region model with a constant R_{CD} under quasi-steady flow. It agreed with the solution of the fully Darcian flow model in the Darcian flow region.

Key words: Confined aquifer; Finite-difference method; Iteration method; Two-region model

Nomenclature

B	aquifer thickness (L)
D_p	characteristic grain diameter (L)
K	hydraulic conductivity of the aquifer (LT^{-1})
K_β	apparent hydraulic conductivity, an empirical constant in the Forchheimer law (LT^{-1})
q	specific discharge in the aquifer (LT^{-1})
q_C	critical specific discharge (LT^{-1})
q_Y , q_N	specific discharges for Darcian flow and non-Darcian flow (LT^{-1}), respectively
Q	well discharge (L^3T^{-1})
s	drawdown (L) for aquifer
s_Y , s_N	drawdowns (L) for Darcian flow and non-Darcian flow, respectively
s_w	drawdown (L) inside well
S	storage coefficient of the aquifer (dimensionless)
r	distance from the center of the well (L)
r_w	radius of the well screen (L)
R_C	critical radius for non-Darcian flow (L)
Re	Reynolds number (dimensionless)
Re_C	critical Reynolds number (dimensionless)
t	pumping time (T)
β	an empirical constant in the Forchheimer law (TL^{-1}), named as inertial force

		coefficient in this study
	ν	kinematic viscosity of the fluid (L^2T^{-1})
	q_{ND}, q_{YD}	dimensionless specific discharges defined in Table 1 in the non-Darcian flow and Darcian flow regions, respectively
	q_{CD}	dimensionless critical specific discharge defined in Table 1
	r_D	dimensionless distance defined in Table 1
	r_{wD}	dimensionless radius of the well screen defined in Table 1
	R_{CD}	dimensionless critical radius defined in Table 1
	s_{ND}, s_{YD}	dimensionless drawdown *s* defined in Table 1 in the non-Darcian flow and Darcian flow regions, respectively
	s_{wD}	dimensionless drawdown inside the well defined in Table 1
	t_D	dimensionless time defined in Table 1
	β_D	dimensionless inertial force coefficient defined in Table 1
	λ	ratio of the hydraulic conductivity and apparent hydraulic conductivity defined in Table 1

The subscript *D* refers to terms in dimensionless form.

The subscripts *N* and *Y* refer to terms related to non-Darcian flow and Darcian flow regions, respectively.

1. Introduction

Darcy's law indicates a linear relationship between the fluid velocity and the hydraulic gradient (Bear, 1972), which is a basic assumption used to handle a great deal of problems related to flow in porous and fractured media. However, many evidences from the laboratory and field experiments show that this linear law may be invalid in some situations, especially when the groundwater flow velocity is sufficiently high or sufficiently low, where non-Darcian flow prevails (Basak, 1977;Bordier and Zimmer, 2000;Engelund, 1953;Forchheimer, 1901;Izbash, 1931;Liu et al., 2012;Soni et al., 1978).

Darcy's law considers kinematic forces but excludes inertial forces of flow. However, the inertia forces become significant with respect to the kinematic forces when the velocity is great, leading to non-Darcian flow (Engelund, 1953;Forchheimer, 1901;Irmay, 1959;Izbash, 1931). Forchheimer (1901) proposed a heuristic Forchheimer law describing the non-Darcian flow, which was an extension of Darcy's law by adding a second-order velocity term, representing the inertial effect. To verify the applicability of the Forchheimer law, many approaches were introduced, such as the dimensional analysis (Ward, 1964), the capillary model (Dullien and Azzam, 1973), the hybrid mixture theory (Hassanizadeh and Gray, 1987), and the volume averaging method (Whitaker, 1996). Recently, Giorgi (1997) and Chen et al. (2001) analytically derived the Forchheimer law from the Navier-Stokes equation. Another widely used model describing the non-Darcian flow was the Izbash equation (Izbash, 1931). This equation was a

fully empirical power-law function obtained through analyzing experimental data. The Izbash equation was preferred for modeling purpose, since the power index in the Izbash equation can be parameterized depending on flow conditions (Basak, 1977). George and Hansen (1992) demonstrated that the Forchheimer and Izbash equations were identical for some cases.

Due to the high velocities, non-Darcian flow is likely to occur near pumping/injecting wells (Yeh and Chang, 2013; Wen et al., 2008b). Several studies showed that the non-Darcian effect had significant influence on hydraulic parameter estimations. For instance, Theis solution cannot be used to explain the pumping test data in the Chaj-Doab area near Gujrat water distributory in Pakistan (Ahmad, 1998), while Birpinar and Sen (2004) and Wen et al. (2011) found that the Forchheimer law worked very well. Quinn et al. (2013) demonstrated that non-Darcian flow effect increased as the initial applied head differential increased in a series of slug tests. Specifically, Quinn et al. (2013) showed that the hydraulic conductivity was underestimated by Darcy's law when the initial applied head differentials were greater than 0.2 m. They pointed out that Darcian flow conditions can be maintained in the sandstone when the initial applied head differentials were less than 0.2 m (Quinn et al., 2013). Mathias and Todman (2010) showed that the Jacob method, based on Darcy's law, cannot fit the step-drawdown tests of van Tonder et al. (2001) when the pumping rate was greater than 10 $m^3 hour^{-1}$. However, the Forchheimer law fitted the step-drawdown tests data very well (Mathias and Todman, 2010). In this study, we will focus on the non-Darcian flow into a pumping well by the Forchheimer law.

Although many efforts have been devoted to study the non-Darcian flow around the well,

the exact solutions have not been obtained due to the non-linearity of the problem (Mathias et al., 2008;Yeh and Chang, 2013). For example, Sen (1990, 2000) employed the Boltzmann transform method to analytically solve the problems related to the non-Darcian flow. This method was showed to be problematic, since both initial and boundary conditions cannot be simultaneously transformed into a form only containing the Boltzmann variable (Camacho and Vasquez, 1992;Wen et al., 2008a). Wen el al. (2008a;2008b) derived the semi-analytical solutions of the non-Darcian flow model by combining the Linearization procedure and the Laplace transform method (LL method), assuming that the flow in the non-Darcian flow region was in quasi-steady state flow. Wen et al. (2008a;2008b) pointed out that solutions by the Boltzmann transform and the LL method coincided at late time. To test the accuracy of the semi-analytical solutions (Wen et al., 2008a;Sen, 2000), Mathias et al. (2008) and Wen et al. (2009) employed the finite-difference method to study the non-Darcian flow problems, and their results showed that the semi-analytical solution only agreed very well with the numerical solution at late pumping stage.

All above-mentioned investigations assume that the non-Darcian flow occurs over the entire domain, which is called a fully non-Darcian flow (F-ND) model hereinafter. In fact, the regime of the flow to the pumping well can be divided into two regions: non-Darcian flow occurs within a narrow region around well, due to the relatively high velocity of flow there, and Darcian flow prevails over the rest domain. One may think that such two-region flow could be described by the Forchheimer law, which would automatically reduce to the Darcy's law at the location far

from the well (because the second-order velocity term in the Forchheimer law will be negligible if velocity approaches zero). However, Forchheimer law (or F-ND model) may not work very well for moderate velocity under which that Darcian flow prevails. Mackie (1983) demonstrated that the two-region model could fit the experimental data in the laboratory better than the F-ND model. Huyakorn and Dudgeon (1976) employed a two-region model to study flow near a pumping well. Basak (1978) presented analytical solutions of the two-region model for steady-state flow to a fully penetrating well. Sen (1988) and Wen et al. (2008b) derived the analytical solutions of the two-region model for transient flow to a pumping well, and both solutions were valid for the groundwater flow in the quasi-steady state.

All researches mentioned above implied that the critical radius is a constant, where the critical radius represents the location separating the non-Darcian and Darcian flows (Sen, 1988;Wen et al., 2008b). For example, the critical radius is infinity for the F-ND model and is zero for the fully Darcian flow model, while it is a finite constant for the two-region model in which the critical radius is determined under the quasi-steady state flow condition (Sen, 1988;Wen et al., 2008b). Actually, the critical radius changes continuously with time for the transient flow, and cannot be determined straightforwardly. For example, the initial critical radius is zero for an initially hydrostatic aquifer, and it gradually increases with time until the system becomes quasi-steady state near a constant-rate pumping well. The movement of critical radius may be more complex for the variable-rate pumping tests (Bear, 1972;Mishra et al., 2012), the slug tests (Quinn et al., 2013) or the step-drawdown tests (Louwyck et al., 2010;Mathias and

Todman, 2010). Therefore, the two-region model with time-dependent critical radius is more reasonable for transient flow near a pumping well, and it is particularly true when the pumping rate changes greatly.

In this study, we will investigate non-Darcian flow into a fully penetrating pumping well considering a time-dependent critical radius using the finite-difference method. A new iteration procedure will be proposed to estimate the moving critical radius. This new model reduces to the F-ND model when the critical radius is infinite and it becomes the fully Darcian flow model when the critical radius is 0.

2. Problem statement and mathematic model

2.1. Location of the critical radius of the two-region model

Previous researches showed that the porous media flow may be divided into four regimes, such as A) non-Darcy pre-linear laminar flow, B) Darcy flow, C) non-Darcy post-linear laminar flow, and D) non-Darcy post-linear turbulent flow (Basak, 1977;Bear, 1972). For radial flow to a pumping well, the velocity in the aquifer decreases with the distance from the well. Therefore, the radial flow might experience all four-flow regimes. To simplify the problem, we use a two-region model that considers a non-Darcian flow region near the well and a Darcian flow region away from the well. A unique feature of the two-region model used in this study is that the critical radius is allowed to vary with time whereas it was assumed to be constant in previous studies (Dudgeon et al., 1972b, a;Huyakorn and Dudgeon, 1976;Mackie, 1983;Sen, 1988;Wen et al., 2008b).

Generally, the start of the non-Darcian flow can be determined by the critical Reynolds number (Re_C), where the Reynolds number is defined as

$$\mathrm{Re}(r,t) = D_p q(r,t)/\nu, \quad (1)$$

where ν is the kinematic viscosity of the fluid (L^2T^{-1}); D_p is the characteristic grain diameter (L); $q(r,t)$ is specific discharge (LT^{-1}) at distance r (L) and time t (T); Re is Reynolds number which depends on time and space (dimensionless). The critical Reynolds number (Re_C) refers to Re at the start of non-Darcian flow. Up to present, there is still considerable debate on Re_C for the initiation of non-Darcian flow in porous media. Scheidegger (1974) gave Re_C to be 0.1 to 75; Zeng and Grigg (2006) suggested the range of Re_C from 1 to 100. Re_C will be set to 100 to make sure non-Darcian flow happen in this study. According to Eq. (1), one can see that the specific discharge is in linear relation to Re. Therefore, the critical specific discharge (q_C) can also be used to determine the start of the non-Darcian flow, since one can calculate q_C for a given Re_C. When the specific discharge is less than or equal to q_C (or $Re \le Re_C$), the flow is considered as Darcian. When the specific discharge is greater than q_C (or $Re > Re_C$), the flow is taken as non-Darcian. Denoting $R_C(t)$ as the critical radius at which $q = q_C$ (or $Re = Re_C$), then it is non-Darcian flow when $r \le R_C(t)$ and Darcian flow when $r > R_C(t)$, as shown in Fig. 1.

For the quasi-steady state flow around a fully penetrating well in a homogeneous and isotropic formation, one has (Sen, 1988;Wen et al., 2008b)

$$R_C = Q/(2\pi B q_C), \quad (2)$$

where B is the thickness of the aquifer (L); Q is the well discharge (L^3T^{-1}). In the case of a

constant pumping rate, R_C is also a constant for a specific Re_C. This constant R_C was used in previous two-region models of transient non-Darcian flow (Sen, 1988;Wen et al., 2008b). Actually, R_C is not a constant for transient flow, and it cannot be determined directly since the velocity distribution changes with time. In this study, a new iteration method will be proposed to determine R_C as described below.

2.2. Mathematic model

Fig. 1 shows the physical model investigated in this study, where a pumping well fully penetrates a confined aquifer. The origin of the cylindrical coordinate system is at the center of the well. The *r*-axis is horizontal and outward from the well, and the *z*-axis is upward vertical. Three assumptions are made in this study. First, the non-Darcian and Darcian flow may coexist and the critical radius is time-dependent, and the non-Darcian flow is governed by the Forchheimer law. Second, the system is hydrostatic before the pumping starts, so $R_C(t=0)$=0. Third, the aquifer is homogeneous, isotropic, infinitely extensive and with a constant thickness. These assumptions, although quite idealized, are standard in well hydraulic study (Papadopulos and Cooper, 1967;Sen, 1988;Wen et al., 2008b). Based on these assumptions, the governing equations of the two-region flow model can be described as follows

$$\frac{\partial q_N(r,t)}{\partial r}+\frac{q_N(r,t)}{r}=\frac{S}{B}\frac{\partial s_N(r,t)}{\partial t}, \text{ if } \ r\le R_C(t), \tag{3}$$

$$\frac{\partial q_Y(r,t)}{\partial r}+\frac{q_Y(r,t)}{r}=\frac{S}{B}\frac{\partial s_Y(r,t)}{\partial t}, \text{ if } \ r> R_C(t), \tag{4}$$

where $s_Y(r,t)$ and $s_N(r,t)$ are drawdowns (L) at distance *r* and time *t* in Darcian flow and non-Darcian flow regions, respectively; *S* is the aquifer storage coefficient (dimensionless).

Initial condition is

$$s_Y(r,0) = s_N(r,0) = 0\,. \tag{5}$$

The outer boundary condition is

$$s_Y(\infty,t) = 0\,. \tag{6}$$

Assuming that the pumping rate is large enough to induce non-Darcian flow near the well, the boundary condition at the wellbore, considering the wellbore storage with a finite diameter well, can be written as

$$2\pi r B q_N(r,t)\Big|_{r\to r_w} - \pi r_w^2 \frac{ds_w(t)}{dt} = -Q\,, \tag{7}$$

where Q is positive for the pumping rate; r_w is the radius of the well (L); s_w is the drawdown inside the well (L). Notice that well loss is not considered so the drawdown is continuous across the well screen

$$s_w(t) = s_N(r_w,t)\,. \tag{8}$$

The drawdown and the discharge from the Darcian flow region into the non-Darcian flow region are continuous at the critical radius

$$s_N\left[R_C(t),t\right] = s_Y\left[R_C(t),t\right], \tag{9}$$

$$q_N\left[R_C(t),t\right] = q_Y\left[R_C(t),t\right]. \tag{10}$$

In the non-Darcian flow region, we use the Forchheimer law to describe the flow (Forchheimer, 1901)

$$q_N + \beta q_N |q_N| = K_\beta \frac{\partial s_N}{\partial r}, \quad (11)$$

in which β (TL^{-1}) and K_β (LT^{-1}) are empirical constants depending on the properties of the medium (Sidiropoulou et al., 2007). K_β is called the apparent hydraulic conductivity and it reduces to the hydraulic conductivity when $\beta = 0$ (Chen et al., 2001;Sidiropoulou et al., 2007). β is called the inertial force coefficient. Many studies demonstrated that the value of β was related to the porous media and the fluid properties (Scheidegger, 1958;Moutsopoulos et al., 2009). For example, Ergun equation (Ergun, 1952) was widely used to estimate β

$$\beta = \frac{1.75 D_p}{150 \nu (1-\phi)}, \quad (12)$$

where ϕ is porosity. When the kinematic viscosity of water (ν) at 20 ℃ is 10^{-6}m^2 s^{-1}, D_p=0.001m, ϕ=0.3, one has $\beta = 2.0 \times 10^{-4}$m^2/day.

In the Darcian flow region, one has

$$q_Y(r,t) = K \frac{\partial s_Y(r,t)}{\partial r}, \quad r > R_c. \quad (13)$$

Eqs. (3) - (13) can be used to describe the groundwater flow in the aquifer with a time-dependent critical radius $R_C(t)$. This new model is an extension of the previous model by Sen (1988). When $R_C(t) \to \infty$, this model becomes the F-ND model. When $R_C(t) = 0$, it reduces to the fully Darcian flow model.

2.3. Dimensionless transformation

Defining the dimensionless variables in Table 1, Eqs. (3) - (13) can be rewritten as

$$\frac{\partial q_{ND}}{\partial r_D}+\frac{q_{ND}}{r_D}=-\frac{\partial s_{ND}}{\partial t_D},\ \ r_D \le R_{CD}, \tag{14}$$

$$\frac{\partial q_{YD}}{\partial r_D}+\frac{q_{YD}}{r_D}=-\frac{\partial s_{YD}}{\partial t_D},\ \ r_D > R_{CD}, \tag{15}$$

$$s_{ND}(r_D,0)=s_{YD}(r_D,0)=0, \tag{16}$$

$$s_{YD}(\infty,t_D)=0, \tag{17}$$

$$s_{ND}[R_{CD}(t_D),t_D]=s_{YD}[R_{CD}(t_D),t_D], \tag{18}$$

$$q_{ND}[R_{CD}(t_D),t_D]=q_{YD}[R_{CD}(t_D),t_D]. \tag{19}$$

Notice that a negative sign has been used for defining q_D in Table 1. The subscript "*D*" means the dimensionless variables. The boundary condition with the wellbore storage (Eq. (7)) in the dimensionless form is

$$\left(r_D q_{ND}\right)\Big|_{r_D\to r_{wD}}+\frac{r_{wD}^2}{2S}\frac{ds_{wD}(t_D)}{dt_D}=1. \tag{20}$$

The dimensionless Forchheimer law becomes

$$q_{ND}+\beta_D q_{ND}|q_{ND}|=-\frac{\partial s_{ND}}{\partial r_D},\ \ r_D \le R_{CD}, \tag{21}$$

where β_D is the dimensionless inertial force coefficient. When the pumping rate is 0.628 $m^3\ s^{-1}$, aquifer thickness is 10 m, and $\beta = 2.0\times10^{-4} m^2/day$, one has β_D =0.02 according to the definition of β_D, as shown in Table 1.

When $r_D > R_{CD}$, groundwater flow follows the Darcy's law in the dimensionless format as

$$q_{YD}(r,t) = -\lambda \frac{\partial s_{YD}}{\partial r_D}, \quad r_D > R_{CD}, \tag{22}$$

where λ is the ratio of the hydraulic conductivity and apparent hydraulic conductivity, and it is usually taken as unity (Sidiropoulou et al., 2007).

3. Numerical solution

Because of the non-linearity of the problem, it is not easy to obtain the analytical solution of drawdown even if $R_{CD}(t_D)$ is constant. In this study, we will employ the finite-difference method to investigate the problem considering a time-dependent $R_{CD}(t_D)$. Due to the axisymmetric nature of the problem, the numerical simulation will be conducted with a non-uniform grid system, where the spatial steps are smaller near the well and become progressively greater away from the well. Similar to previous studies (Mathias et al., 2008;Wen et al., 2009), we discretize the dimensionless space r_D logarithmically. The dimensionless space domain [r_{wD}, r_{eD}] is discretized into N nodes excluding the two boundary nodes r_{wD} and r_{eD}, where r_{eD} is a relatively large dimensionless distance used to approximate the infinite boundary (Mathias et al., 2008;Wen et al., 2009). For any node of r_i, $r_{wD}<r_i<r_{eD}$, i=1, 2…N, one has

$$r_i = (r_{i-1/2} + r_{i+1/2})/2, \qquad i=1, 2\ldots N, \tag{23}$$

where $r_{i+1/2}$ is calculated as follows

$$\log_{10}(r_{i+1/2}) = \log_{10}(r_{wD}) + i\left[\frac{\log_{10}(r_{eD}) - \log_{10}(r_{wD})}{N}\right], \; i=0, 1\ldots N. \tag{24}$$

After spatial discretization, Eqs. (14) - (15) become

$$\frac{ds_{YD,i}}{dt_D} \approx \frac{r_{i-1/2}q_{YD,i-1/2} - r_{i+1/2}q_{YD,i+1/2}}{r_i\left(r_{i+1/2} - r_{i-1/2}\right)},\ i=2, 3\ldots N_s\text{-}1,\ \ r_D \le R_{CD}, \tag{25}$$

$$\frac{ds_{ND,i}}{dt_D} \approx \frac{r_{i-1/2}q_{ND,i-1/2} - r_{i+1/2}q_{ND,i+1/2}}{r_i\left(r_{i+1/2} - r_{i-1/2}\right)},\ i= N_s, 3\ldots N\text{-}1,\ \ r_D > R_{CD}, \tag{26}$$

where $q_{YD,i}$ and $s_{YD,i}$ are the dimensionless specific discharge q_{YD} and dimensionless drawdown s_{YD} at node i for the Darcian flow, respectively; $q_{ND,i}$ and $s_{ND,i}$ are the dimensionless specific discharge q_{ND} and dimensionless drawdown s_{ND} at node i for the non-Darcian flow, respectively. In terms of the Forchheimer equation of Eq. (21), one can obtain

$$q_{ND,i-1/2} \approx \frac{1}{2\beta_D}\left\{-1+\left[1+4\beta_D\left(\frac{s_{ND,i-1} - s_{ND,i}}{r_i - r_{i-1}}\right)\right]^{\frac{1}{2}}\right\},\ \ i=2, 3\ldots N_s\text{-}1, \tag{27}$$

and

$$q_{ND,i+1/2} \approx \frac{1}{2\beta_D}\left\{-1+\left[1+4\beta_D\left(\frac{s_{ND,i} - s_{ND,i+1}}{r_{i+1} - r_i}\right)\right]^{\frac{1}{2}}\right\},\ \ i=2, 3\ldots N_s\text{ -}1, \tag{28}$$

where node N_s means the location of $R_{CD}\left(t_D\right)$. At the well-aquifer boundary, one has

$$q_{ND,1-1/2} \approx \frac{1}{2\beta_D}\left\{-1+\left[1+4\beta_D\left(\frac{s_{wD} - s_{ND,1}}{r_1 - r_{wD}}\right)\right]^{\frac{1}{2}}\right\}, \tag{29}$$

where s_{wD} is the dimensionless drawdown inside the well. Considering Eq. (20), s_{wD} can be approximated as follows

$$\frac{ds_{wD}}{dt_D} \approx \frac{2S}{r_{wD}^2}\left(1 - r_{wD}q_{ND,1-1/2}\right). \tag{30}$$

When $r_D > R_{CD}$, the finite-difference scheme of the specific discharge can be obtained from Eq. (22)

$$q_{YD,i-1/2} \approx \lambda \frac{s_{YD,i-1} - s_{YD,i}}{r_i - r_{i-1}},\ i= N_s, N_s+1 \ldots N\text{-}1, \tag{31}$$

$$q_{YD,i+1/2} \approx \lambda \frac{s_{YD,i} - s_{YD,i+1}}{r_{i+1} - r_i},\ i= N_s, N_s+1 \ldots N\text{-}1. \tag{32}$$

As for the boundary at the infinity, the finite-difference scheme is

$$q_{YD,N+1/2} \approx \lambda \frac{s_{YD,N}}{r_{eD} - r_N}. \tag{33}$$

Now one obtains a set of ordinary differential equations. It is notable that R_{CD} or N_s which is related to the index *i* in Eqs. (27) - (28) and Eqs. (31) - (32) is time-dependent. In the following section, a new iteration method will be proposed to determine the values of R_{CD} or N_s.

4. Iteration method to determine R_{CD} or N_s

Before introducing the new iteration method, the relationship between R_{CD} and the velocity distribution will be investigated first, based on the two-region model with a constant R_{CD}. The values of the constant R_{CD} are set to 0, 0.02, 0.04, 0.08 and 0.50, respectively. The other parameters are $r_{wD} = 1\times10^{-4}$, $\beta_D = 20$, $\lambda = 1$. The mathematic model with a constant R_{CD} will be solved by the finite-difference method.

Fig. 2a shows the specific discharge distributions with different R_{CD} of 0, 0.02, 0.04, 0.08 and 0.50. The curve of R_{CD} =0 represents the fully Darcian flow model. One can find that the

specific discharge decreases with increasing R_{CD} at a given r_D, starting from its maximum at R_{CD}=0 (Darcian flow). This observation is understandable. The increasing R_{CD} implies a stronger contribution of the inertial effect, which also means a larger resistance to flow, thus it leads to a smaller specific discharge. After trying many different sets of aquifer parameters, such as β_D=0.002, 0.02, 0.2, and R_{CD} = 0.01, 0.03, 0.1, numerical simulation indicates that this observation is universally valid. This observation will serve as the basis for the new iteration method to seek the location of $R_{CD}(t_D)$.

Similar to the use of Re_C to determine the start of the non-Darcian flow, one can use q_{CD} for the initiation of the non-Darcian flow, where q_{CD} is the dimensionless critical specific discharge defined in Table 1. We denote r_{jCD} as the newly computed critical radius at the j^{th} step of the new iteration method, where $j = 1,2,3\cdots$. Since the aquifer system is initially hydrostatic, the initial critical radius r_{0CD} is set to 0. For a given dimensionless time t_{1D}, the detailed procedures of the iteration method for searching $R_{CD}(t_{1D})$ will be introduced as follows. Firstly, the specific discharge distribution in the aquifer can be calculated using Eqs. (25) - (33) with $R_{CD}(t_{1D}) = r_{0CD}$, as shown in Fig. 2b. Based on the computed specific discharge distribution, one can find the new critical radius r_{1CD} according to a given constant q_{CD}. Secondly, the new specific discharge distribution can be similarly calculated using Eqs. (25) - (33) with $R_{CD}(t_{1D}) = r_{1CD}$, and the new critical radius r_{2CD} can be obtained according to q_{CD}. It is notable that r_{1CD} and r_{2CD} serve as the upper and lower limits for searching $R_{CD}(t_{1D})$, as illustrated in Fig. 2b. Similarly, one can estimate the new critical radius r_{3CD} using r_{2CD}, where r_{3CD} is

located somewhere between r_{1CD} and r_{2CD}. Following the same procedures, a new critical radius r_{4CD} can be calculated based on r_{3CD}, and r_{4CD} is between r_{2CD} and r_{3CD}. One can repeat above computations until the new critical radius finally converges. For the actual problems, we define a convergence criterion $\left|R_{CD}^{old} - R_{CD}^{new}\right| \le \xi$, where R_{CD}^{old} and R_{CD}^{new} are the critical radius for the previous step and present step, respectively; ξ is a small positive value such as 0.001. If this criterion is satisfied, the new critical radius r_{jCD} is thought as the estimation of $R_{CD}(t_{1D})$. We develop a MATLAB program named as Two-Region Model with Moving critical radius (MTRM) to facilitate the computation. By the way, this iteration method is convergent. Fig. 3 represents the flow chart of the MTRM algorithm, where t_k is the time at time step k; k_{max} is the total number of the time steps; dt_D is the dimensionless time step; $s_{D,i}$ and $q_{D,i}$ are the dimensionless specific drawdown and dimensionless discharge at node i in the aquifer respectively.

5. Results and discussions

5.1. Comparison with the previous solutions

To test the new solution, the fully Darcian flow solution of Papadopoulos and Cooper (1967), the fully non-Darcian flow solution of Mathias et al. (2008) and the two-region model of Sen (1988) will be introduced. Figs. 4a and 4b show the distance-drawdown curves of the four mentioned-above models in the early and late pumping stages, respectively. In these two figures, "Papadopoulos and Cooper (1967)" represents the analytical solution of the fully Darcian flow model, "Sen (1988)" is the analytical solution of the two-region model by the Boltzmann

transform method, and "Mathias et al. (2008)" represents the numerical solution of the fully non-Darcian flow model. The deflection point of the curve is the location of the critical radius.

In the early stage, the differences among three previous solutions and the new solution of this study are obvious, as shown in Fig. 4a. Firstly, the solution of Papadopoulos and Cooper (1967) is smaller than the others near the well. This is because the inertial forces of the non-Darcian flow increase the resistance for flow, thus resulting in drawdown greater than those for the Darcian flow near the well. The second is that the F-ND solution agrees with the new solution near the well. The third is that the solution of Sen (1988) does not agree with the new solution near the well at the early time. This is probably because of the Boltzmann transform method used by Sen (1988) to deal with the non-Darcian flow at the early time, which has been discussed in several previous studies (Camacho and Vasquez, 1992;Wen et al., 2008b). The fourth is that there is a deflection point on the new solution, leading to discontinuity of the drawdown slope. This observation may be reasonable, as also reported by Moutsopoulos et al. (2009), who named it non-uniform hydraulic behavior.

In the late pumping stage, the transient flow approaches the quasi-steady state, and the specific discharge distribution is invariant with time according to Eqs. (3) - (4) or Eqs. (14) - (15), regardless of the Darcian flow or non-Darcian flow. Under the quasi-steady state flow condition, the critical radius obtained by this new solution becomes a constant which is the same as the one used by previous two-region models such as Sen (1988) and Wen et al. (2009). Therefore, the new solution agrees with that of Sen (1988) very well at late time (see Fig. 4b). Another fact that

can be seen in Fig. 4b is that the new solution agrees with the solution of Papadopoulos and Cooper (1967) in the Darcian flow region.

5.2 Effect of the inertial force coefficient to the critical radius

The inertial force coefficient (β) is of primary concern for the non-Darcian flow described by the Forchheimer equation, and the values of β_D are chosen as 0.001, 0.01, and 0.1. Fig. 5 shows the critical radius (R_{CD}) changes with time for different dimensionless inertial force coefficients. Several observations can be seen. Firstly, R_{CD} increases with time until the flow approaching the quasi-steady state condition. In the early pumping stage, the specific discharge is very large near the well and decreases quickly with the distance from the well, so R_{CD} is very small. With time going, the cone of depression will expand along the radial direction and the slope of the cone of depression becomes flatter, so R_{CD} becomes greater. Secondly, a larger β_D would reduce the rate of change R_{CD} versus time, thus result in longer time to approach its asymptotic value, and consequently leads to a smaller R_{CD} at a specific time in the transient state (see Fig. 5). This is because a larger β_D implies a stronger inertial force, which increases the resistance of flow. The third interesting observation is that the asymptotic value of R_{CD} is the same for different β_D . This can be explained using Eq. (2). Based on the definition of the dimensionless parameters defined in Table 1, Eq. (2) becomes

$$q_{CD} = 1/R_{CD} . \tag{34}$$

Therefore, the value of R_{CD} does not depend on β_D under the quasi-state state flow condition, while it only reciprocally depends on the critical specific discharge.

5.3 Effect of the critical specific discharge to the critical radius

The criterion to judge the initiation of the non-Darcian flow is an important factor of concern. Up to now, there is still considerable debate on what value of Re_C to use for the start of non-Darcian low. The recommended values of Re_C range from 0.1 to 100 for porous media flow (Bear, 1972;Scheidegger, 1974;Zeng and Grigg, 2006). To check the influence of Re_C on R_{CD} during the transient flow, the values of q_{CD} are chosen as 100, 50 and 10 considering the direct relationship of q_{CD} and R_{CD} in Eq. (2). The other parameters are β_D =0.01, and $r_{wD} = 1\times10^{-4}$.

Fig. 6 shows the effect of q_{CD} on R_{CD}. It is obvious that the asymptotic value of R_{CD} is equal to $1/q_{CD}$, as reflected in Eq. (34). Another interesting observation is that R_{CD} decreases with increasing q_{CD}, and it takes shorter time for R_{CD} to approach its asymptotic value.

5.4. Type curves in the non-Darcian flow region and Darcian flow region

Type curves are a series of curves that reveal the functional relationship between the well functions (or drawdown) and the dimensionless time factors (Sen, 1988;Wen et al., 2011). Type curve is one of the common approaches to identify the aquifer parameters or to predict the drawdown(Sen, 1988;Wen et al., 2011). Sen (1988) presented different type curves in the Darcian flow region and non-Darcian flow region based on a two-region model. In that model (Sen, 1988), R_{CD} was a fixed value which only depends on the rate of pumping but independent of time. In this study, R_{CD} changes with time, and the type curves might be different from the ones generated by Sen (1988). To investigate the behaviors of the type curves of the new

solution, the two observation locations will be chosen, r_D=0.005 and 0.02. According to Eq. (34), the maximum of R_{CD} is 0.001 at the quasi-steady state, so the flow at r_D=0.005 will experience both Darcian flow (at the early time) and non-Darcian flow (at late time), while the flow at r_D=0.02 is always Darcian.

Fig. 7 shows the time-drawdown at r_D=0.005 for different dimensionless inertial force coefficients in the log-log scale. Two interesting observations can be seen from this figure. The first observation is that there is a deflection point in the curve of β_D =0.1 or 1, that becomes larger in time with increasing β_D. This is because a larger β_D implies a stronger inertial effect, which leads to a larger drawdown and longer time to approach the quasi-steady state condition. This observation is not found in the F-ND model (Wen et al., 2011) and in the two-region model (Sen, 1988). The second observation is that the drawdown in the quasi-steady state increases with increasing β_D, and the reason for this has been explained in previous studies (Wen et al., 2011).

Fig. 8 represents the time-drawdown at r_D=0.02 in the log-log scale. One notable point is that flow at r_D=0.02 is always Darcian, so there is no deflection point in the type curves. The differences among the curves with different β_D are obvious at the beginning, and then they approach the same value at the quasi-steady state.

6. Summary and conclusions

In this study, a new two-region flow model considering the time-dependent critical radius (R_{CD}) is established to investigate the groundwater flow into a pumping well, and a new iteration

method is proposed to estimate R_{CD}, based on the finite-difference method. Results show that this iteration method is convergence although it has not been analytical verified using rigorous mathematic model. In the non-Darcian flow region, the flow is governed by the Forchheimer equation, and the start of the non-Darcian flow is determined by the critical specific discharge, which is calculated by the critical Reynolds number. The new solution is compared with previous solutions, such as the fully Darcian flow model, the two-region model with a constant critical radius, and the fully non-Darcian flow model. The impacts of the dimensionless inertial force coefficient (β_D) and dimensionless critical specific discharge (q_{CD}) on the critical radius and flow field have been analyzed. Several findings can be drawn from this study:

(1) In the early stage, the new solution agrees with the fully non-Darcian flow solution near the well, differs with the fully Darcian flow model of Papadopoulos and Cooper (1967) and the two-region model of Sen (1988).

(2) In the quasi-steady flow stage, the new solution agrees with the solution of Sen (1988) very well. It agrees very well with the solution of the fully Darcian flow model (Papadopulos and Cooper, 1967) in the Darcian flow region.

(3) R_{CD} increases with time until reaching the quasi-steady state flow, and the asymptotic value of R_{CD} only depends on q_{CD}. A larger β_D would reduce the rate of change of R_{CD} with time, and result in a smaller R_{CD} at a specific time during the transient flow state.

(4) There is a deflection point in the type curve when the observation well location is within the non-Darcian flow region in the quasi-steady state when $\beta_D \geq 0.1$, and the time associated

with this deflection point becomes larger with a larger β_D.

Acknowledgments

This research was partially supported by Program of the National Basic Research Program of China (973) (No. 2011CB710600, 2011CB710602), National Natural Science Foundation of China (No. 41172281, 41372253), the scholarship to Quanrong Wang from China Scholarship Council, Field Demonstration of Integrated Monitoring Program of Land and Resources in Middle Yangtze River Jianghan-Dongtin Plain (1212011120084), and Study on Groundwater Resources and Environmental Problems in Middle Yangtze River Jianghan-Dongtin Plain (No. 1212011121142). We thank two anonymous reviewers for the critical and constructive comments that help us improve this manuscript.

References

Ahmad, N.: Evaluation of groundwater resources in the upper middle part of Chaj-Doak area, Pakistan., PhD, Istanbul Technical Univ., Turkey, 1998.

Basak, P.: Non-penetrating well in a semi-infinite medium with nonlinear flow, Journal of Hydrology, 33, 375-382, 10.1016/0022-1694(77)90047-6, 1977.

Basak, P.: Analytical solutions for two-regime well flow problems, Journal of Hydrology, 38, 147-159, 1978.

Bear, J.: Dynamics of fluids in porous media., Elsevier, New York, 1972.

Birpinar, M., and Sen, Z.: Forchheimer groundwater flow law type curves for leaky aquifers, Journal of Hydrologic Engineering, 9, 51-59, doi:10.1061/(ASCE)1084-0699(2004)9:1(51), 2004.

Bordier, C., and Zimmer, D.: Drainage equations and non-Darcian modelling in coarse porous media or geosynthetic materials, Journal of Hydrology, 228, 174-187, 10.1016/s0022-1694(00)00151-7, 2000.

Camacho, R. G., and Vasquez, M.: Analytical solution incorporating nonlinear radial flow in confined aquifers - comment, Water Resources Research, 28, 3337-3338, 10.1029/92wr01646, 1992.

Chen, Z. X., Lyons, S. L., and Qin, G.: Derivation of the Forchheimer law via homogenization, Transport in Porous Media, 44, 325-335, 10.1023/a:1010749114251, 2001.

Dudgeon, C. R., Huyakorn, P. S., and Swan, W. H. C.: Hydraulics of flow near wells in unconsolidated sediments, Field studies, The university of new south wales, Australia, 1972a.

Dudgeon, C. R., Huyakorn, P. S., and Swan, W. H. C.: Hydraulics of flow near wells in unconsolidated sediments, Theoretical and experimental studies, The university of new south wales, Australia, 1972b.

Dullien, F. A. L., and Azzam, M. I. S.: Flow rate pressure gradient measurements in periodically nonuniform capillary tubes, Aiche Journal, 19, 222-229, 10.1002/aic.690190204, 1973.

Engelund, F.: On the laminar and turbulent flows of ground water through homogeneous sand, Tech. Univ. Denmark, Copenhagen, Denmark, 1953.

Ergun, S.: Fluid flow through packed columns, Chemical engineering progress, 48, 89-94, 1952.

Forchheimer, P. H.: Wasserbewegung durch boden, Zeitsch-rift des Vereines Deutscher Ingenieure, 49, 1736-1749, 1901.

George, G. H., and Hansen, D.: Conversion between quadratic and power law for non-Darcy Flow, Journal of Hydraulic Engineering-Asce, 118, 792-797, 10.1061/(asce)0733-9429(1992)118:5(792), 1992.

Giorgi, T.: Derivation of the Forchheimer law via matched asymptotic expansions, Transport in Porous Media, 29, 191-206, 10.1023/a:1006533931383, 1997.

Hassanizadeh, S. M., and Gray, W. G.: High-velocity flow in porous-media, Transport in Porous Media, 2, 521-531, 1987.

Huyakorn, P., and Dudgeon, C. R.: Investigation of 2-regime well flow, Journal of the hydraulics division-asce, 102, 1149-1165, 1976.

Irmay, S.: On the theoretical derivations of Darcy and Forchheimer formulas - discussion - reply, Journal of Geophysical Research, 64, 486-487, 10.1029/JZ064i004p00486, 1959.

Izbash, S. V.: O filtracii V Kropnozernstom Materiale, Leningrad, USSR (in Russian), 1931.

Liu, H. H., Li, L. C., and Birkholzer, J.: Unsaturated properties for non-Darcian water flow in clay, Journal of Hydrology, 430, 173-178, 10.1016/j.jhydrol.2012.02.017, 2012.

Louwyck, A., Vandenbohede, A., and Lebbe, L.: Numerical analysis of step-drawdown tests: Parameter identification and uncertainty, Journal of Hydrology, 380, 165-179, 10.1016/j.jhydrol.2009.10.034, 2010.

Mackie, C. D.: Determination of Nonlinear formation losses in pumping wells, International Conference on Groundwater and Man, 5-9 December 1983.

Mathias, S. A., Butler, A. P., and Zhan, H. B.: Approximate solutions for Forchheimer flow to a well, Journal of Hydraulic Engineering-Asce, 134, 1318-1325, 10.1061/(asce)0733-9429(2008)134:9(1318), 2008.

Mathias, S. A., and Todman, L. C.: Step-drawdown tests and the Forchheimer equation, Water Resources Research, 46, W0751410.1029/2009wr008635, 2010.

Mishra, P. K., Vessilinov, V., and Gupta, H.: On simulation and analysis of variable-rate pumping tests, Ground Water, 51, 469-473, 10.1111/j.1745-6584.2012.00961.x, 2012.

Moutsopoulos, K. N., Papaspyros, I. N. E., and Tsihrintzis, V. A.: Experimental investigation of inertial flow processes in porous media, Journal of Hydrology, 374, 242-254, http://dx.doi.org/10.1016/j.jhydrol.2009.06.015, 2009.

Papadopulos, I. S., and Cooper, H. H.: Drawdown in a well of large diameter, Water Resources Research, 3, 241-244, 10.1029/WR003i001p00241, 1967.

Quinn, P. M., Parker, B. L., and Cherry, J. A.: Validation of non-Darcian flow effects in slug tests conducted in fractured rock boreholes, Journal of Hydrology, 486, 505-518, 10.1016/j.jhydrol.2013.02.024, 2013.

Scheidegger, A. E.: The physics of flow through porous media, Soil Science, 86, 355, 1958.

Scheidegger, A. E.: The physics of flow through porous media, University of Toronto Press, 152-170 pp., 1974.

Sen, Z.: Type curves for two-region well flow, Journal of Hydraulic Engineering, 114, 1461-1484, 10.1029/WR024i004p00601, 1988.

Sen, Z.: Nonlinear radial flow in confined aquifers toward large-diameter wells, Water Resources Research, 26, 1103-1109, 10.1029/WR026i005p01103, 1990.

Sen, Z.: Non-Darcian groundwater flow in leaky aquifers, Hydrological Sciences Journal-Journal Des Sciences Hydrologiques, 45, 595-606, 10.1080/02626660009492360, 2000.

Sidiropoulou, M. G., Moutsopoulos, K. N., and Tsihrintzis, V. A.: Determination of Forchheimer equation coefficients a and b, Hydrological Processes, 21, 534-554, 10.1002/hyp.6264, 2007.

Soni, J. P., Islam, N., and Basak, P.: A experimental evaluation of non-Darcian flow in porous media, Journal of Hydrology, 38, 231-241, 10.1016/0022-1694(78)90070-7, 1978.

van Tonder, G. J., Botha, J. F., and van Bosch, J.: A generalised solution for step-drawdown tests including flow dimension and elasticity, Water S.A, 27, 345-354, 2001.

Ward, J. C.: Turbulent flow in porous media, Journal of Hydraulics Division, American Society of Civil Engineers, 90, 1-12, 1964.

Wen, Z., Huang, G. H., and Zhan, H. B.: An analytical solution for non-Darcian flow in a confined aquifer using the power law function, Advances in Water Resources, 31, 44-55, 10.1016/j.advwatres.2007.06.002, 2008a.

Wen, Z., Huang, G. H., Zhan, H. B., and Li, J.: Two-region non-Darcian flow toward a well in a confined aquifer, Advances in Water Resources, 31, 818-827, 10.1016/j.advwatres.2008.01.014, 2008b.

Wen, Z., Huang, G. H., and Zhan, H. B.: A numerical solution for non-Darcian flow to a well in a confined aquifer using the power law function, Journal of Hydrology, 364, 99-106, 10.1016/j.jhydrol.2008.10.009, 2009.

Wen, Z., Huang, G. H., and Zhan, H. B.: Non-Darcian flow to a well in a leaky aquifer using the Forchheimer equation, Hydrogeology Journal, 19, 563-572, 10.1007/s10040-011-0709-2, 2011.

Whitaker, S.: The Forchheimer equation: A theoretical development, Transport in Porous Media, 25, 27-61, 10.1007/bf00141261, 1996.

Yeh, H.-D., and Chang, Y.-C.: Recent advances in modeling of well hydraulics, Advances in Water Resources, 51, 27-51, 10.1016/j.advwatres.2012.03.006, 2013.

Zeng, Z. W., and Grigg, R.: A criterion for non-Darcy flow in porous media, Transport in Porous Media, 63, 57-69, 10.1007/s11242-005-2720-3, 2006.

Table 1 Dimensionless variables used in this study

$r_D = \frac{r}{B}$	$r_{wD} = \frac{r_w}{B}$
$R_{CD} = \frac{R_C}{B}$	$t_D = \frac{K_\beta t}{SB}$
$\beta_D = \frac{Q\beta}{2\pi B^2}$	$\lambda = \frac{K}{K_\beta}$
$s_{wD} = \frac{2\pi K_\beta B}{Q} s_w$	$s_{YD} = \frac{2\pi K_\beta B}{Q} s_Y(r,t)$
$s_{ND} = \frac{2\pi K_\beta B}{Q} s_N(r,t)$	$q_{ND} = -\frac{2\pi B^2}{Q} q_N(r,t)$
$q_{YD} = -\frac{2\pi B^2}{Q} q_Y(r,t)$	$q_{CD} = -\frac{2\pi B^2}{Q} q_C$

Figure captions

Fig. 1. The schematic diagram of the non-Darcian flow into a fully penetrating pumping well considering the time-dependent critical radius.

Fig. 2a. Specific discharge distributions with different critical radius R_{CD}.

Fig. 2b. The schematic diagram showing the iterative process of seeking R_{CD}.

Fig. 3. Flow chat of the MTRM algorithm.

Fig. 4a. Comparison of the distance-drawdowns by the fully Darcian flow model (Papadopoulos and Cooper, 1967), the fully non-Darcian flow model (Mathias et al., 2008), the two-region flow model (Sen, 1988), and the new model in early pumping stage.

Fig. 4b. Comparison of the distance-drawdowns by the fully Darcian flow model (Papadopoulos and Cooper, 1967), the fully non-Darcian flow model (Mathias et al., 2008), the two-region flow model (Sen, 1988), and the new model in late pumping stage.

Fig. 5. Time-dependent critical radius (R_{CD}) for different values of the inertial force coefficient β_D .

Fig. 6. Time-dependent critical radius (R_{CD}) for different values of the critical specific discharge.

Fig. 7. Time-drawdown at r_D=0.005 for different inertial force coefficients in a log-log scale.

Fig. 8. Time-drawdown at r_D=0.02 for different inertial force coefficients in a log-log scale.

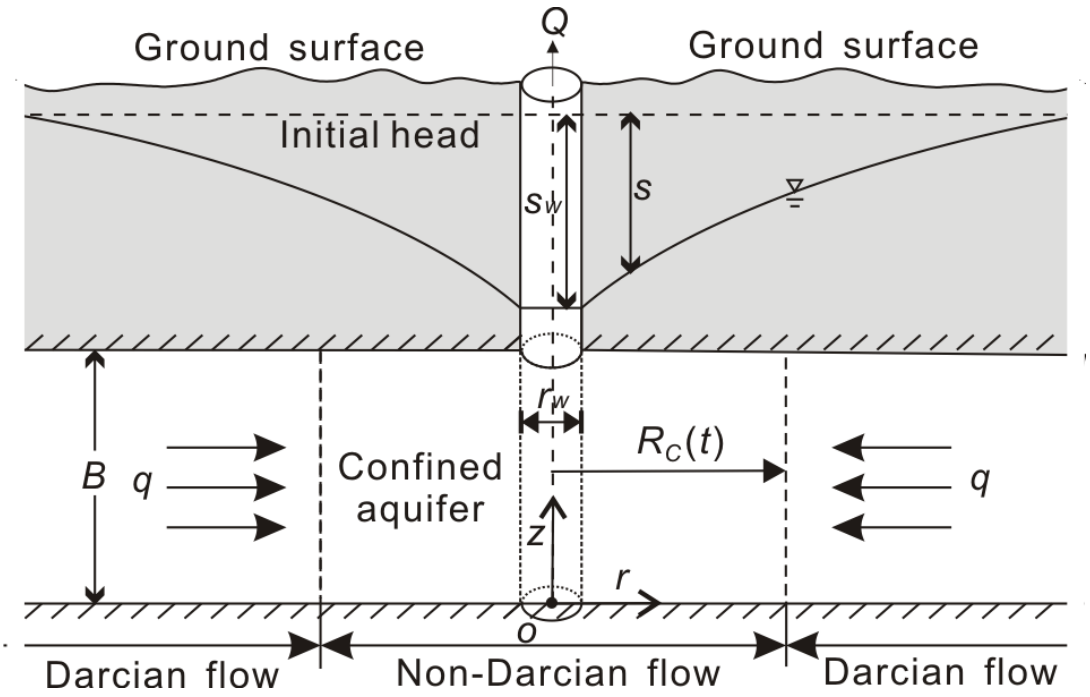
Q
Ground surface
Ground surface
Initial head
s_w
s
r_w
$R_C(t)$
B
q
Confined
aquifer
q
z
r
o
Darcian flow
Non-Darcian flow
Darcian flow

Fig. 1.

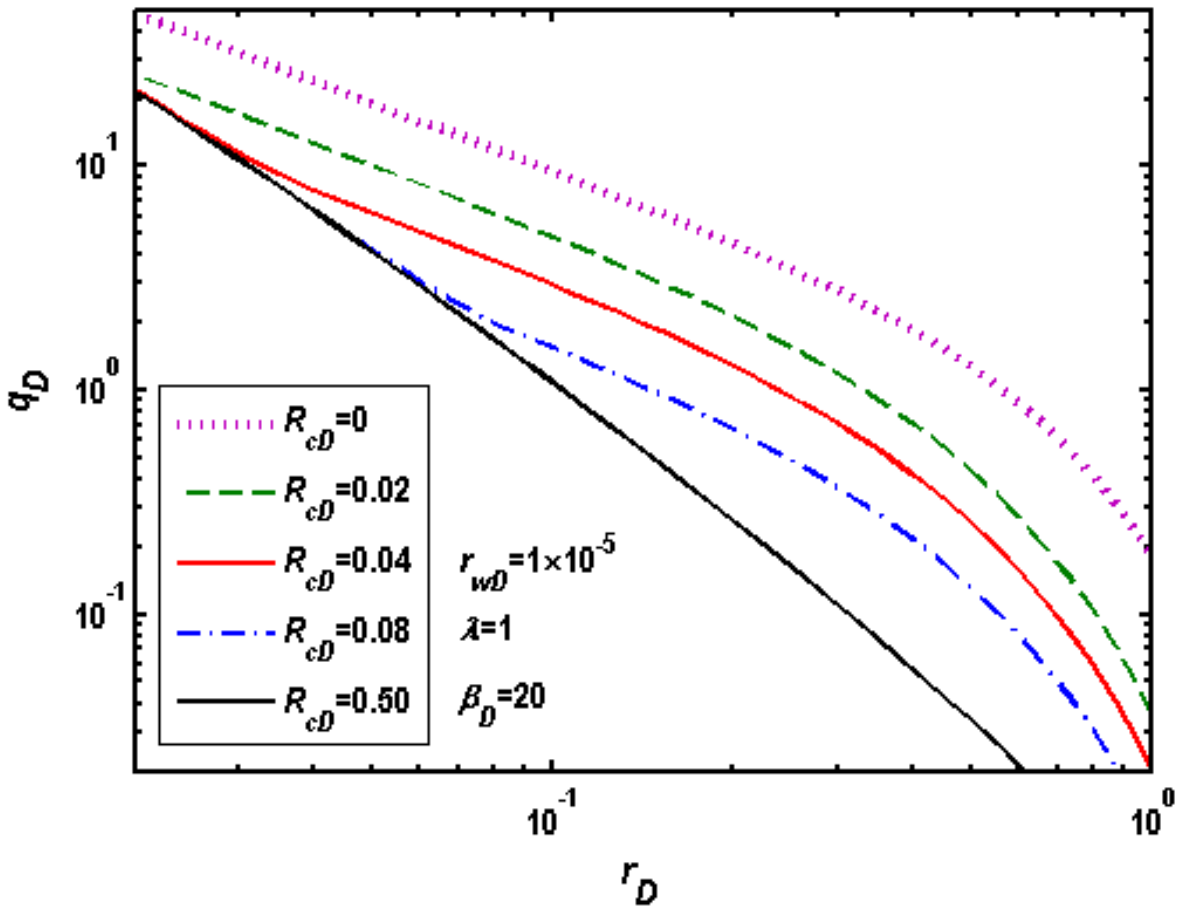
q_D
r_D
10^{1}
10^{0}
10^{-1}
10^{-1}
10^{0}
R_{cD}=0
R_{cD}=0.02
R_{cD}=0.04
R_{cD}=0.08
R_{cD}=0.50
r_{wD}=1×10^{-5}
λ=1
β_D=20

Fig. 2a.

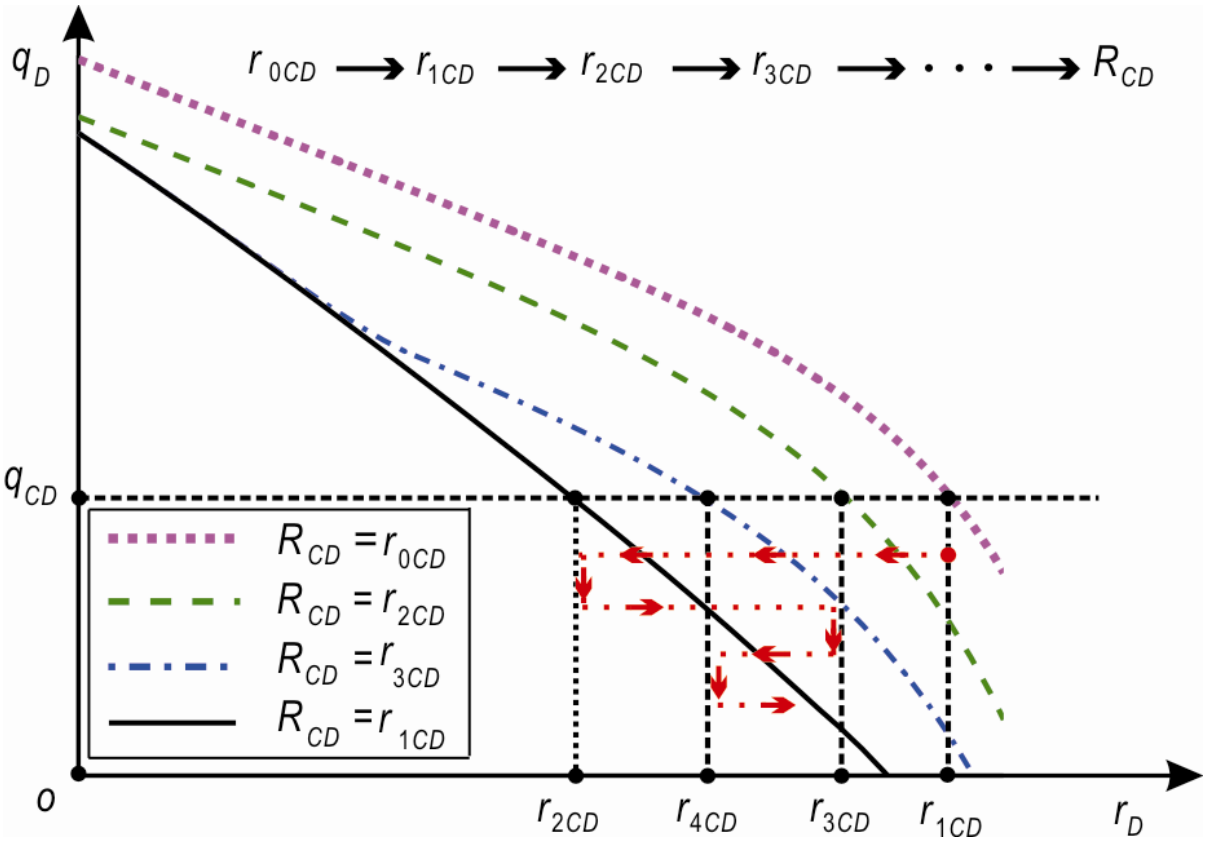
q_D
$r_{0CD} \rightarrow r_{1CD} \rightarrow r_{2CD} \rightarrow r_{3CD} \rightarrow \cdots \rightarrow R_{CD}$
q_{CD}
$R_{CD} = r_{0CD}$
$R_{CD} = r_{2CD}$
$R_{CD} = r_{3CD}$
$R_{CD} = r_{1CD}$
o
r_{2CD}
r_{4CD}
r_{3CD}
r_{1CD}
r_D

Fig. 2b.

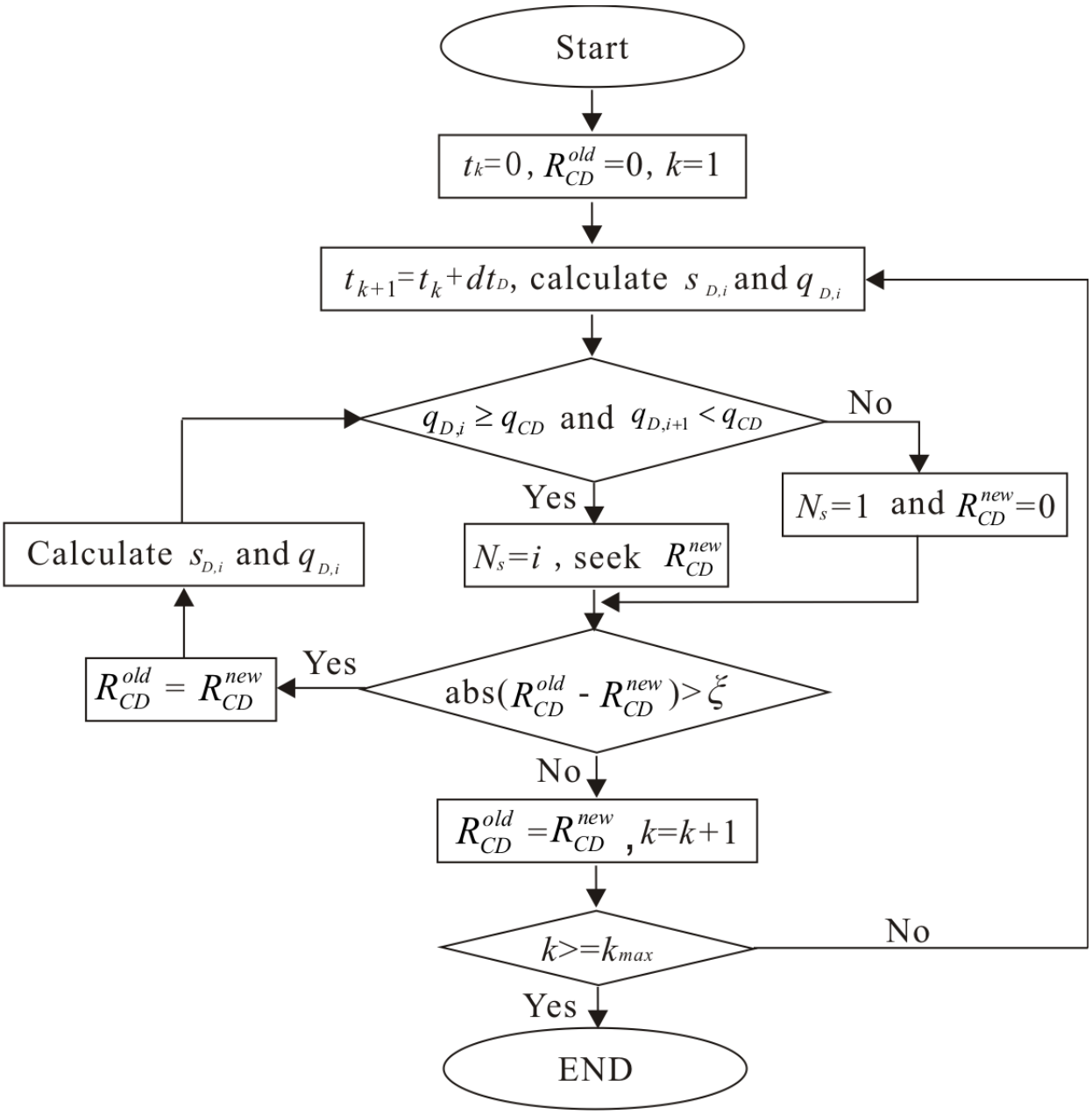
Start
$t_k=0,\ R_{CD}^{old}=0,\ k=1$
$t_{k+1}=t_k+dt_D$, calculate $s_{D,i}$ and $q_{D,i}$
$q_{D,i} \geq q_{CD}$ and $q_{D,i+1} < q_{CD}$
No
Yes
$N_s=1$ and $R_{CD}^{new}=0$
$N_s=i$, seek R_{CD}^{new}
Calculate $s_{D,i}$ and $q_{D,i}$
$R_{CD}^{old} = R_{CD}^{new}$
Yes
$\text{abs}(R_{CD}^{old} - R_{CD}^{new}) > \xi$
No
$R_{CD}^{old} = R_{CD}^{new}$, $k=k+1$
$k>=k_{max}$
No
Yes
END

1

2 Fig. 3.

3

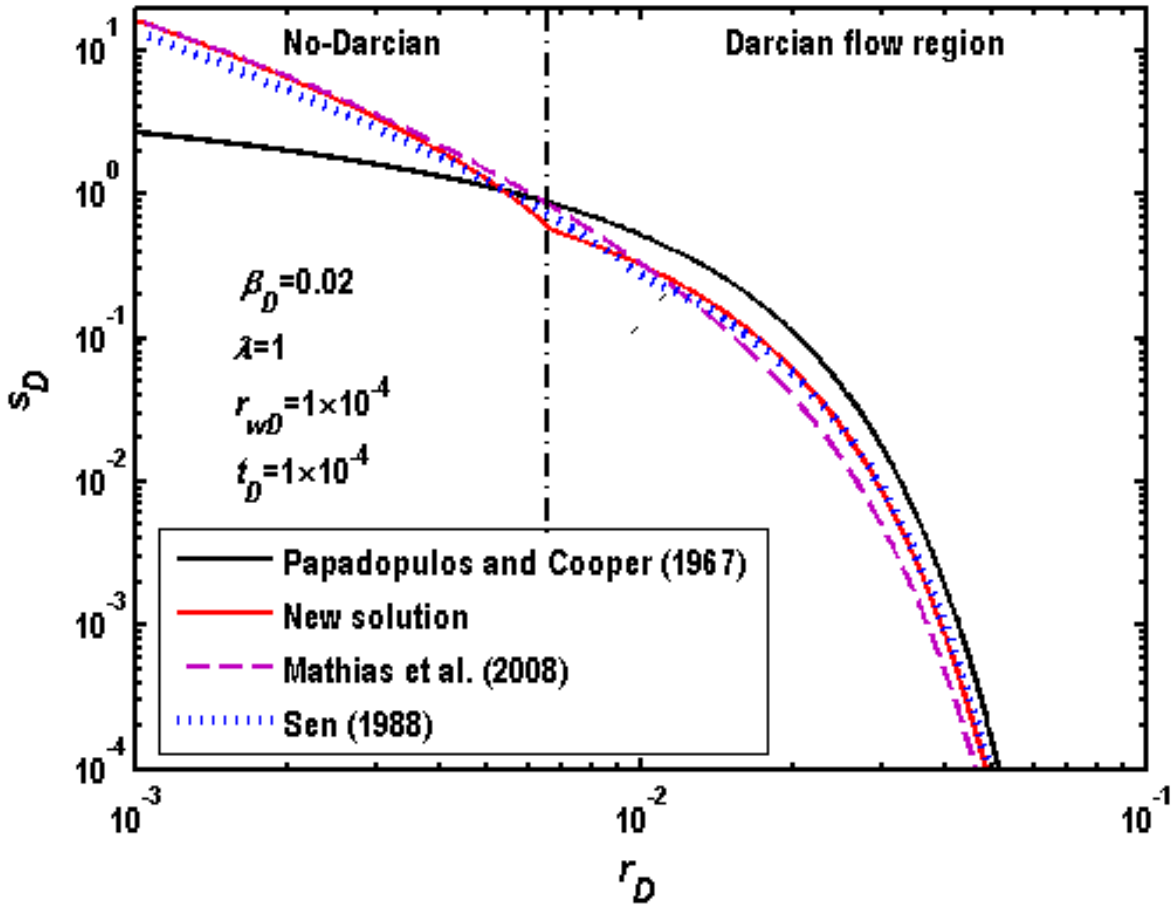
No-Darcian
Darcian flow region
β_D=0.02
λ=1
r_{wD}=1×10^{-4}
t_D=1×10^{-4}
Papadopulos and Cooper (1967)
New solution
Mathias et al. (2008)
Sen (1988)
s_D
r_D
10^{1}
10^{0}
10^{-1}
10^{-2}
10^{-3}
10^{-4}
10^{-3}
10^{-2}
10^{-1}

Fig. 4a.

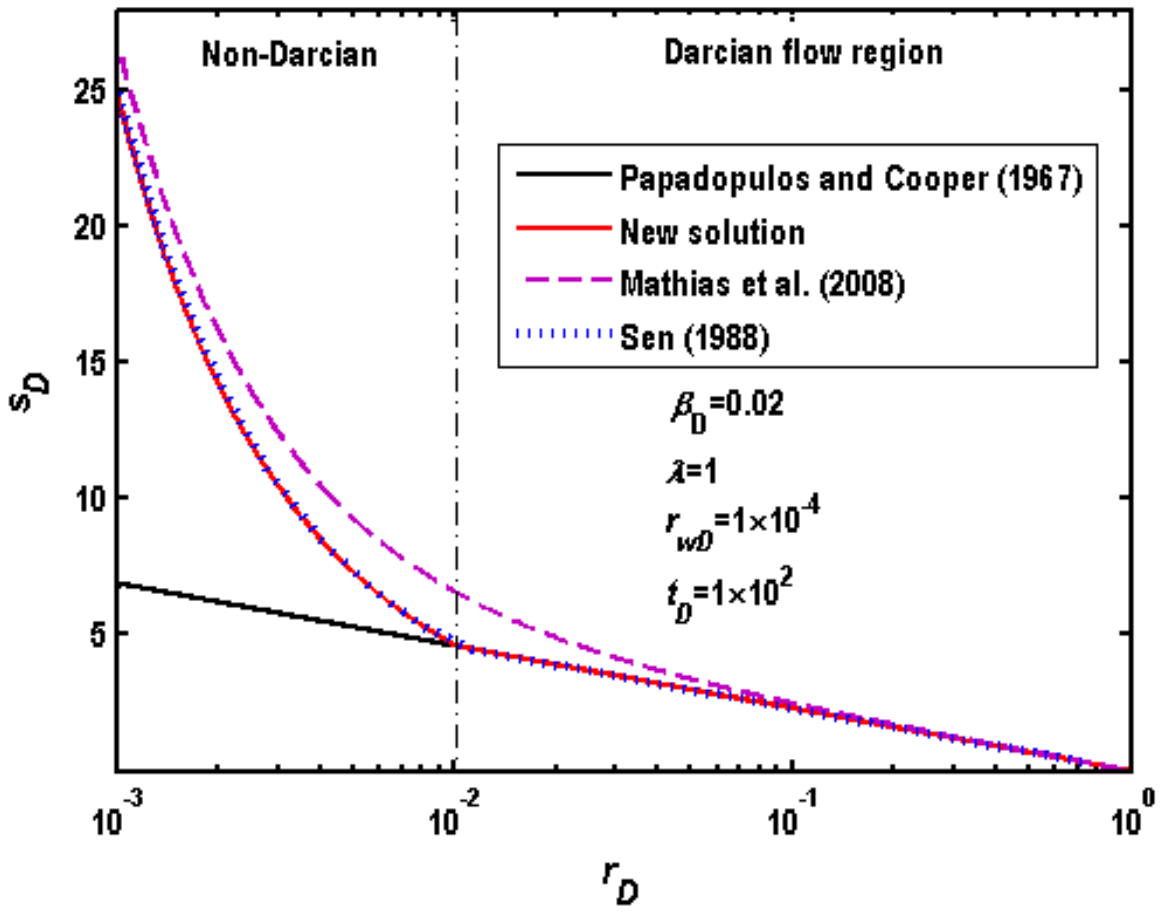
Non-Darcian
Darcian flow region
Papadopulos and Cooper (1967)
New solution
Mathias et al. (2008)
Sen (1988)
β_D=0.02
λ=1
r_{wD}=1×10^{-4}
t_D=1×10^2
s_D
r_D
25
20
15
10
5
10^{-3}
10^{-2}
10^{-1}
10^0

1

2 Fig. 4b.

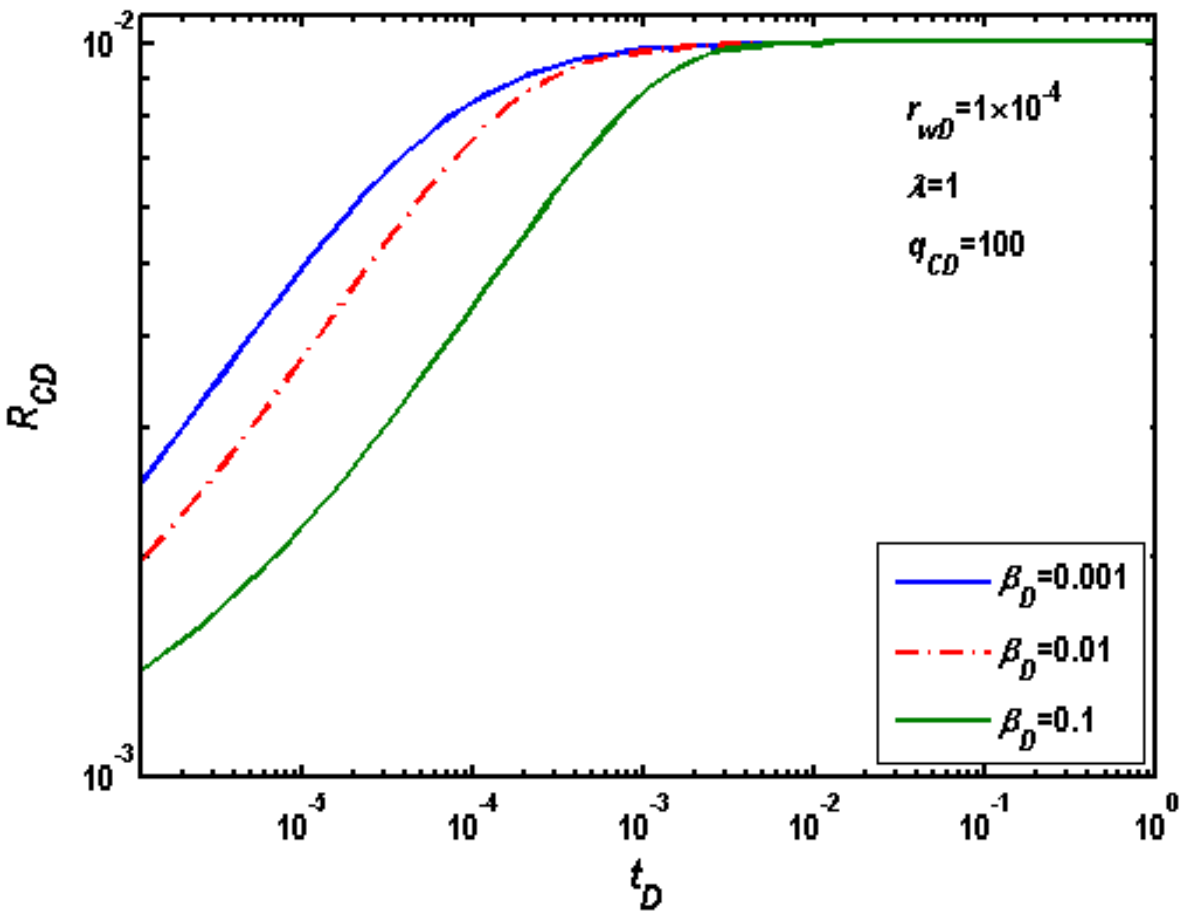
10^{-2}
10^{-3}
R_{CD}
r_{wD}=1×10^{-4}
λ=1
q_{CD}=100
β_D=0.001
β_D=0.01
β_D=0.1
10^{-5}
10^{-4}
10^{-3}
10^{-2}
10^{-1}
10^{0}
t_D

1

2 Fig. 5.

3

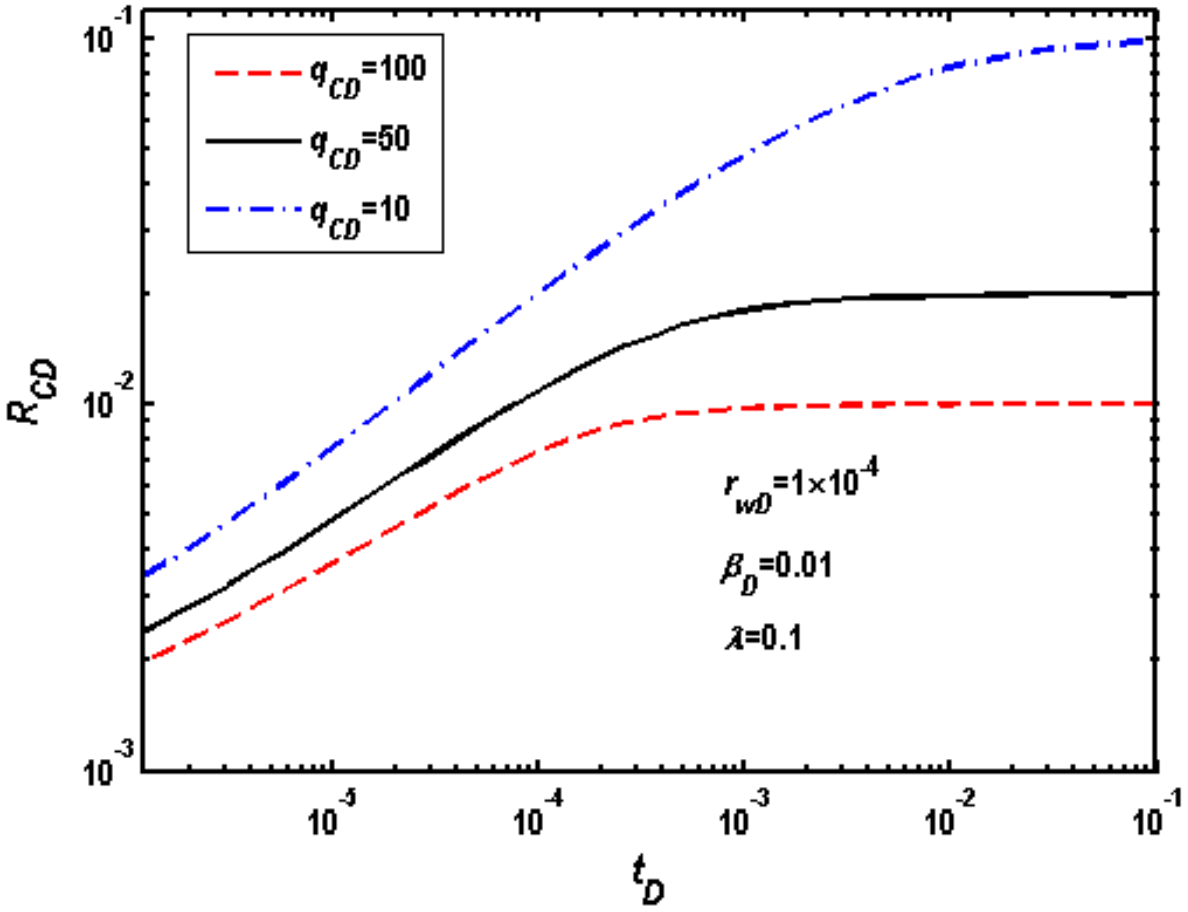
q_{CD}=100
q_{CD}=50
q_{CD}=10
r_{wD}=1×10^{-4}
β_D=0.01
λ=0.1
R_{CD}
t_D
10^{-1}
10^{-2}
10^{-3}
10^{-5}
10^{-4}
10^{-3}
10^{-2}
10^{-1}

1

2 Fig. 6.

3

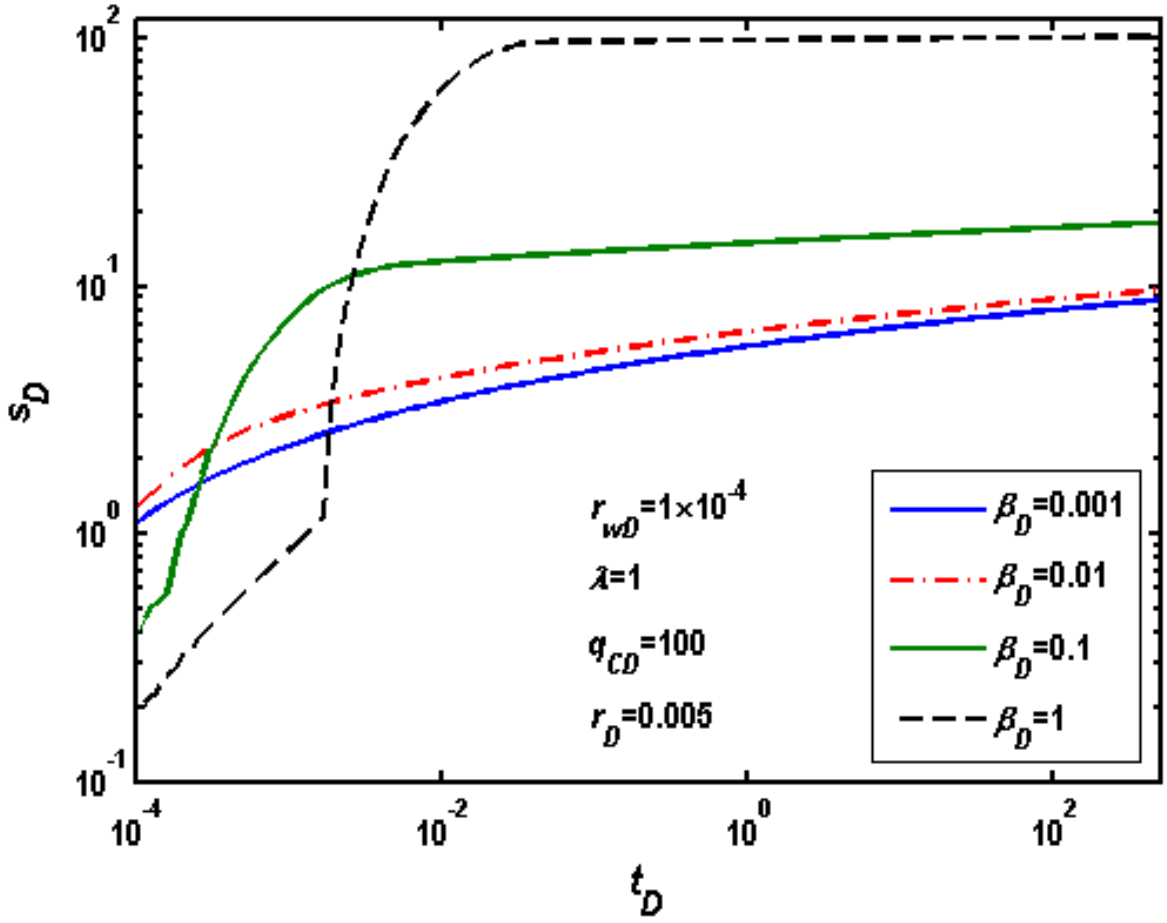
10^2
10^1
10^0
10^{-1}
s_D
10^{-4}
10^{-2}
10^0
10^2
t_D
r_{wD}=1×10^{-4}
λ=1
q_{CD}=100
r_D=0.005
β_D=0.001
β_D=0.01
β_D=0.1
β_D=1

1

2 Fig. 7.

3

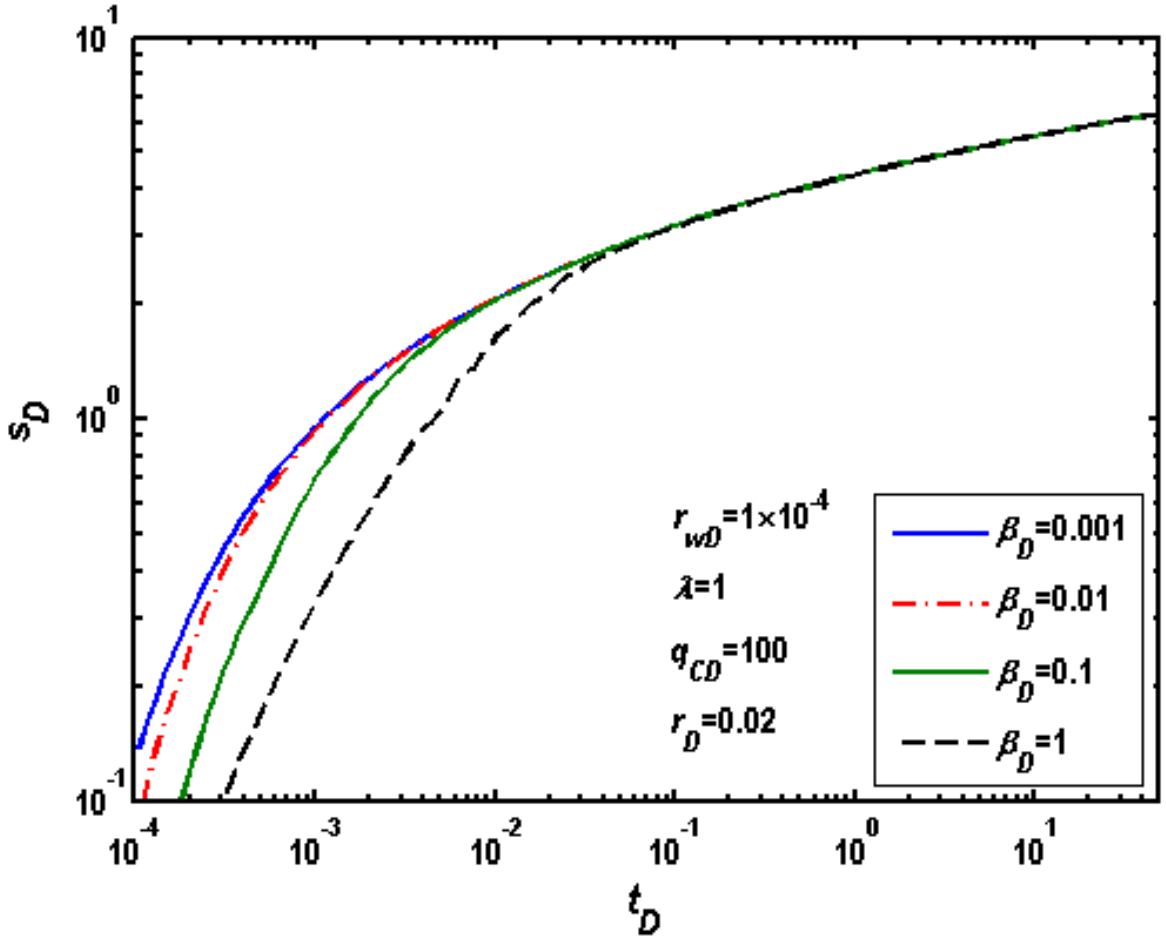
10^{1}
10^{0}
10^{-1}
s_D
10^{-4}
10^{-3}
10^{-2}
10^{-1}
10^{0}
10^{1}
t_D
r_{wD}=1×10^{-4}
λ=1
q_{CD}=100
r_D=0.02
β_D=0.001
β_D=0.01
β_D=0.1
β_D=1

1

2 Fig. 8.